Elimination Mechanisms. Deuteroxide/Hydroxide Isotope Effects as a Measure of Proton Transfer in the Transition States for E2 Elimination of 2-(*p*-Trimethylammoniophenyl)ethyl 'Onium Ions and Halides. Mapping of the Reaction-Coordinate Motion[1]

Donald A. Winey and Edward R. Thornton*

Contribution from the Department of Chemistry, University of Pennsylvania, Philadelphia, Pennsylvania 19174. *Received June 29, 1974*

Abstract: Deuteroxide/hydroxide kinetic isotope effects for the compounds *p*-$(CH_3)_3N^+C_6H_4CH_2CH_2X$ with various leaving groups X, whose syntheses are described herein, were determined at 60°, as follows (X, k_{DO^-}/k_{HO^-}): $N^+(CH_3)_3$, 1.62 ± 0.12; $N^+(CH_3)_2C_6H_5$, 1.68 ± 0.02; $S^+(CH_3)_2$, 1.54 ± 0.02; F, 1.66 ± 0.03; Cl, 1.40 ± 0.03; Br, 1.30 ± 0.02. These isotope effects are best interpreted as measuring different extents of proton transfer from C_β to the attacking lyoxide ion in the concerted E2 transition state, and thus provide a series ranging from more-than-half transfer (isotope effects greater than ca. 1.41, the square root of the maximal isotope effect, ca. 2.0, for complete transfer) to less-than-half transfer. It is also suggested that the data available for E2 reactions best fit transition states which are E1cB-like for poor leaving groups and nearly central for good leaving groups. Significant perpendicular as well as parallel effects in the transition state geometry changes associated with structural changes in reactants explain the data, including the shift to E1cB-like transition states with poor leaving groups, which is considered to be the origin of the Hofmann and Saytzev orientation rules. A "force formulation" of a previously proposed theory of structural effects upon transition-state geometries is also outlined, as a clarification and aid to application of the theory.

The E2 elimination mechanism (eq 1) is one of the most

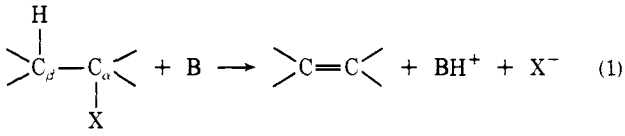

(1)

extensively studied because of the interesting possibilities for stereochemistry, orientation, and substituent effects.[2] The possibility of variable transition states differing in RP character (reactant-like:product-like) as well as carbanion (at C_β) or carbonium ion (at C_α) character has presented an extraordinary mechanistic challenge,[3-8] to which many investigators have responded.

A major question is the degree of proton transfer from C_β to the base B at the transition state, and the way in which this degree of proton transfer will change with different reactants. The Westheimer Effect,[9] which suggests that the primary hydrogen isotope effect for the proton being transferred from C_β should reach a maximum at half-transfer and should be lower for more or for less than half-transfer, makes the otherwise attractive tool of primary isotope-effect measurement difficult to interpret fully. Since isotope effects provide a key to probing transition state structure while keeping that structure [i.e., the ENG (equilibrium nuclear geometry) of the transition state] constant,[10] we adopted the idea of using DO^- vs. HO^- as bases to explore the degree of proton transfer.[1a] Since the resulting secondary isotope effects k_{DO^-}/k_{HO^-} are expected to increase with increasing degree of proton transfer to the lyoxide ion, up to a maximum value of ca. 2 for complete transfer,[1a,10-13] the degree of proton transfer could be measured. The proton was found to be substantially transferred in the case of β-phenylethylammonium and sulfonium ions,[1a] and a great deal of P character was independently demonstrated by the fact that the primary isotope effects for the transferred proton tended to be weaker for larger k_{DO^-}/k_{HO^-}.

With the experimental evidence then available and a simple perturbation theory of the effects of structural changes upon transition-state geometries,[14] we proposed that the transition-state reaction-coordinate motion for E2 reactions involves mainly proton transfer from C_β to the base, with relatively little stretching of the C_α–X bond.[1a] The mechanism suggested is still concerted E2, and the C_α–X bond is considered to be around half broken at the transition state, but the completion of C_α–X bond breaking is pictured as occurring after the transition state rather than as part of the imaginary vibration of the transition state. This hypothesis led to a prediction that increasing P character would tend to increase carbanion character at C_β, while increasing R character would tend to increase carbonium ion character at C_α.

It was first pointed out by Bunnett[4] that this transition state and the predictions following from it were inconsistent with the amounts of 1-ene and 2-enes formed in eliminations from 2-hexyl halides.[15]

It has become clear that, in contrast with our earlier assumptions,[1a] the vast amount of more recent data requires parallel and perpendicular effects to be comparable in magnitude, as suggested also by More O'Ferrall's potential-energy diagrams.[5] In fact, with that assumption, Smith and Bourns have recently pointed out[16] that agreement with known data follows if one also assumes that halides and other compounds with good leaving groups have central[3] transition states, while 'onium ions and other compounds with poor leaving groups have E1cB-like transition states as we had suggested.[1a] This idea is further supported by the prediction[1a,5,14] that an increasingly poor leaving group should shift transition state structure in the E1cB-like direction. Indeed, all data, including structural changes in base, leaving group, and at the α- and β-carbon atoms, and probes of proton transfer, carbanion character, π character, and leaving group departure, now appear to be consistent with these transition-state structures.

We can therefore conclude with considerable confidence that the abundance of data, taken together, provides a mapping of the transition-state structures and reaction-coordinate motions. Since the trend from central to E1cB-like transition states with poorer leaving groups nicely explains trends in yields of less- and-more substituted olefins, we can further conclude that the main basis of the Saytzev and

Hofmann orientation rules resides in central and E1cB-like transition-state structures, respectively. These structures suggest that the Hofmann transition state probably has considerable development of π character, but this is outweighed in determining relative rates and products by the substantial carbanion character.

A probe of the connection between halide and 'onium leaving groups is of considerable interest, and the k_{DO^-}/k_{HO^-} effect seems especially useful, in that it provides a measure of the extent of proton transfer to base. Interestingly, it is predicted that the extent of proton transfer to base will increase for poor leaving groups until, as the E1cB-like extreme is approached, it will be little affected by further changes to poorer leaving groups.

We have therefore synthesized and measured deuteroxide isotope effects for 2-(*p*-trimethylammoniophenyl)ethyl bromide, chloride, fluoride, dimethylsulfonium ion, dimethylanilinium ion, and trimethylammonium ion, the ionic *p*-trimethylammonio group providing sufficient water solubility for all substrates. The observed isotope effects correspond well with the above prediction.

Results

The substrates, with *p*-toluenesulfonate (tosylate, TsO^-) present as the counterion of the trimethylammonio substituent, were studied by titration of aliquots. Rate constants are reported in Table I. Yields of olefin were within experimental error of 100% (±4%) for all substrates.

In addition to the isotope effect associated with neutralization of lyoxide ions, which is known to make DO^- a stronger base than HO^- by a factor of approximately 2, there is a solvent (solvation) isotope effect associated with the change from H_2O to D_2O.[10,13] Such a solvation isotope effect might result, for example, from different solvation of the leaving group in the transition state than in the reactants and thus contribute to the experimentally observed isotope effects. If this effect were important, then the observed isotope effects would contain its contribution and might not truly reflect the degree of neutralization of the lyoxide ion in the transition state. Therefore, some experiments were carried out with phenoxide as base. For the bromide substrate, the rate constants were independent of concentration of excess phenol, giving $k = 253 \pm 4$ and $270 \pm 4 \times 10^{-5}$ l. mol^{-1} sec^{-1} at 60° in H_2O and D_2O, respectively, with average olefin yields of 52 ± 1% and 54 ± 1%, respectively. From this information, values of k_{D_2O}/k_{H_2O} for phenoxide are calculated to be 1.11 ± 0.07 for E2 and 1.03 ± 0.07 for SN2. For the dimethylsulfonium substrate, rate constants were dependent on excess phenol concentration, giving extrapolated rate constants at $(\text{phenol})^{-1} = 0$ of 3.58 and 4.47×10^{-5} l. mol^{-1} sec^{-1} for H_2O and D_2O, respectively. The olefin yield was 100%, and $k_{D_2O}/k_{H_2O} = 1.25 \pm 0.08$. There will be rapid α-deuterium exchange into the sulfonium substrate; therefore, this isotope effect includes any secondary α isotope-effect contribution as well. In view of the substantial error limits resulting from the above experimental complexities, these phenoxide isotope effects mainly indicate that the solvent isotope-effect contributions are rather small.

The isotope effects are given in Table II, along with previous[1a] results.

Discussion

The secondary lyoxide isotope effects measure the extent of bond formation between lyoxide oxygen and β proton at the transition state.[1a,10-13] This is essentially a Brϕnsted catalysis relationship so that, for zero bond formation, k_{DO^-}/k_{HO^-} should equal unity and, for full bond formation, k_{DO^-}/k_{HO^-} should equal the ratio of equilibrium basicities of DO^- and HO^-, for which literature values average 2.0.[13] For partial bond formation, the isotope effect should be 2.0^{β}, where β is the Brϕnsted coefficient and is a measure of the fraction of bond formation; therefore, a half-formed bond should have an isotope effect of $2.0^{0.5} = 1.4$. Such Brϕnsted type relationships among isotope effects are actually much more reliable than the usual Brϕnsted relationships among bases of different structures, because the bases differing only by isotope substitution have virtually identical electronic structures, and thus the isotope effects are for two reactions which proceed on exactly the same electronic potential-energy surface. These conclusions can be justified by statistical mechanical calculations showing the origin of the isotope effect.[10,13]

Table I. Rate Constants for the E2 Reaction of p-$(TsO^-)Me_3N^+-C_6H_4-CH_2CH_2X$ and LO^- at 60°

X	Solvent[a]	$k \times 10^5$, l. mol^{-1} sec^{-1} [b]
Br	H_2O	1238 ± 7
	D_2O	1611 ± 11
Cl	H_2O	61.91 ± 0.62
	D_2O	86.47 ± 0.75
F	H_2O	3.653 ± 0.016
	D_2O	6.075 ± 0.072
$^+SMe_2$	H_2O	514.0 ± 1.0
	D_2O	793.4 ± 2.0
$^+NMe_2C_6H_5$	H_2O	159.6 ± 1.3
	D_2O	268.1 ± 0.3
$^+NMe_3$	H_2O	51.29 ± 1.30[c]
	D_2O	83.05 ± 4.05[c]

[a] Base is the conjugate base of the solvent. [b] Each rate constant is the average of three or more runs with standard deviation. [c] Large standard deviation due to experimental difficulty of removing trimethylamine on a rotary evaporator prior to titration of each kinetic point.

Therefore, bond formation between lyoxide oxygen and β proton is more complete with 'onium ions than halides (except fluoride) and is probably more than half complete for the 'onium ions and fluoride, approximately half complete for chloride, and less than half complete for bromide. For transition states with extensive O-H bond formation, the isotope effects appear to be relatively little affected by changes of leaving group, but, for those with less extensive O-H bond formation, the isotope effects increase significantly as the leaving group is made poorer. Experimental error is such that one cannot distinguish a significant trend in comparing the present isotope effects for substrates with the *p*-ammonio substituent and prior[1a] data for corresponding substrates with *p*-H substituent. The new results demonstrate a continuity of varying transition-state structure with respect to formation of the O-H bond as the leaving group is changed and thus show the connection between 'onium- and halide-type leaving groups.

Transition-State Mapping. The goal of science is to fit models to facts, in the case of reaction mechanism studies to fit a structural model of the transition state to the data. Structural interpretation of rate data is necessarily approximate, but one can hope to map the transition-state structure by looking for *trends*—a trend being a quantity with a specified direction but an unspecified magnitude. Given enough data on trends, it should be possible to do the sort of "curve-fitting" or mapping suggested for E2 reactions, in which transition states are located qualitatively on a potential-energy surface by requiring that the predictions for the given transition state structure fit the observed trends.[5,6,14,17]

Correctness of Predictions. One can derive predictions for transition-state structural trends from consideration of potential-energy surfaces[5,6,17] or from consideration of per-

Table II. Secondary Isotope Effects in Elimination Reactions of β-Phenylethyl Derivatives with Lyoxide Ions

X in p-$(CH_3)_3N^+C_6H_4CH_2CH_2X$	k_{DO^-}/k_{HO^-}, 60°	Rel rate, H_2O, 60°	X in $C_6H_5CH_2CH_2X$	k_{DO^-}/k_{HO^-}, 80.45°	Rel rate, H_2O, 80.45°
$N^+(CH_3)_3$	1.62 ± 0.12	14	$N^+(CH_3)_3$	1.79 ± 0.04	(1)
$N^+(CH_3)_2C_6H_5$	1.68 ± 0.02	44	$N^+(CH_3)_2C_6H_5$	1.62 ± 0.04	5
$S^+(CH_3)_2$	1.54 ± 0.02	140	$S^+(CH_3)_2$	1.57 ± 0.04	23
F	1.66 ± 0.03	(1)			
Cl	1.40 ± 0.03	17			
Br	1.30 ± 0.02	340			

turbations of single transition-state structures.[14] These predictions are necessarily the same; the construction of a surface nicely allows one to select cross-sections parallel and perpendicular to the reaction-coordinate motion of the transition state, make predictions based on the perturbation theory,[14] and then incorporate these predictions into a prediction of how the surface will change with a given change in reactant structure. It may be asked how one can be sure the predictions are correct. This question was raised by Saunders and Cockerill,[2] who showed that E2 data agree with all "unambiguous" predictions made by the perturbation theory[1a,14] but expressed concern over the predictions for, e.g., different charge types. Therefore, we summarize here an improved method which is conceptually easier to apply. This is a so-called "force formulation", in which it is recognized that geometric changes in ENG's (equilibrium nuclear geometries), be they transition states or stable species, result entirely from the perturbing effects of forces induced upon the nuclei if one makes a structural change, causing the nuclei to relax to a new ENG. This formulation follows immediately from the previous theory[14] since the force is simply the negative slope of energy with respect to geometric change. It is possible to make predictions of such forces, based on well-studied stereoelectronic considerations, which will be usually agreed to be unambiguous. It should be emphasized that such predictions are easily made because they are not being made for an arbitrary, unknown structure; the predictions are made for a given model structure, which is well defined, and the question to be asked is whether the observed data fit those predictions and therefore fit that model.

Force Formulation. (1) A structural change will exert a force on the nuclei and thus displace the ENG.

(2) For each normal mode of true vibration, the ENG will be shifted in the direction of the net force on the nuclei closest to the site of structural change (or most affected by the structural change).

(3) For a reaction coordinate normal mode, the ENG will be shifted in the direction *opposite* to the net force on the nuclei closest to the site of structural change (or most affected by the structural change).

(4) The shift in ENG is larger when the effective force constant for the normal mode is nearer zero. In a transition state, normal modes involving mainly the motions of nuclei which are in reacting (partial) bonds [i.e., the reaction coordinate and antireaction coordinate(s)] will have effective force constants near zero. Therefore, these nuclei and these normal modes will be the ones which are most affected by the structural change. The net force can be made zero or near-zero by opposing effects within a single normal mode, as when more than one nucleus is affected, but in opposite directions.

(5) The shift in ENG is the *sum* of the separate effects on the normal modes.

Explicitly, in ref 14, the perturbing force is simply $-m$ (cf. eq 1), and the perturbed ENG is at $-m/k$, where k is the force constant (cf. eq 3). Therefore for a true vibration ($k > 0$), the ENG shift is positive for a positive force but, for a reaction-coordinate motion ($k < 0$), the ENG shift is negative for a positive force. The summation over normal coordinates is demonstrated both in terms of energies and in terms of forces (eq 5-8) in ref 14.

σ bonding is well approximated as resulting from relatively localized electron pairs. If a structural change is made which changes one of the nuclei involved in the normal mode under investigation, changes in electronegativity and possibly even in charge type may result. However, it is mainly the changes in covalent bonding (rather than electrostatic effects resulting from changes in charge type) which should determine the forces in most cases, provided there is a significant amount of covalent character in the bond. For example, if we change from chloride to trimethylamine as leaving group in an E2 reaction and consider the force between C_α and the leaving group, the substitution of trimethylamine in the place of chloride in the transition-state geometry of the chloride will introduce an attractive force between nitrogen and carbon since nitrogen overlaps more effectively than chlorine and thus forms stronger covalent bonds to carbon than does chlorine. Because of effects 2 and 3 above, the reaction coordinate must be considered separately from true vibration. For a central reaction coordinate, according to 3, the bond between C_α and leaving group will be most affected by the structural change, and the fact that this bond is only partial in the transition state means that the force effect will be greater than in the reactant. Therefore, *relative* to the reactant, the transition state will have a C_α-N bond which is shifted in the direction opposite to the force, i.e., the C_α-N bond in the transition state will be more completely broken than the C_α-Cl bond in the corresponding transition state. All of the other nuclei which move in the reaction-coordinate motion will shift correspondingly to a more product-like geometry; the proton, for example, will tend to be more completely transferred from C_β. The effects of the true vibrations must be added onto the above effect, however, according to 5, and the results depend on the nature of the reaction coordinate. Furthermore, in a mechanism such as this, where the transition state involves several reacting bonds, it may be difficult to predict the effects on the more remote reacting bonds. In such cases, the potential-energy surfaces of More O'Ferrall[5] provide a simple and elegant way of approximating the answer.

Predictions for E2 Mechanisms. Since predictions may be different for different transition-state models, one cannot make a single prediction for the E2 mechanism. As mentioned in the introductory section, Smith and Bourns[16] suggest that substrates with good leaving groups react via central transition states, in which the reaction-coordinate motion involves simultaneous proton transfer and leaving-group departure. On the other hand,[16] the data require that substrates with poor leaving groups react via E1cB-like transition states and further require that the reaction-coordinate motion involves mainly proton transfer (the carbon-leaving group bond is partially broken in the transition state but is not being further broken as part of the reaction-coordinate motion, and further breakage occurs only after the

transition state has been traversed).[1a,16]

These models can be used as the basis for predicting a variety of structural effects according to the force formulation. We will restrict ourselves to four such effects since these are the major ones which have been studied experimentally. (1) A poorer leaving group will exert a force in the direction of shortening the C_α-X bond if inserted into the transition-state geometry characteristic of some better leaving group; therefore, in a given transition-state model, any normal mode which involves a change in the C_α-X bond length (corresponding to a horizontal component in Figure 1) will be increased or decreased according to whether it is the reaction coordinate or a true vibration, and the transition state for the case of the poorer leaving group will occur at the resultant of these effects. (2) A stronger base will exert a force in the direction of more complete proton transfer, thus tending to lengthen the C_β-H bond, if inserted into the transition-state geometry characteristic of some weaker base; therefore, in a given transition-state model, any normal mode which involves a change in amount of proton transfer (corresponding to a vertical component in Figure 1) will be increased or decreased, as described in case 1. (3) An EWG (electron-withdrawing group, carbanion stabilizing) at C_β will exert a force in the direction of increased carbanion character if inserted into the transition-state geometry characteristic of some lesser EWG; therefore, in a given transition-state model, any normal mode which involves a change in carbanion character (corresponding to a component along the *diagonal* extending between the C^- and C^+ corners in Figure 1) will be increased or decreased, as described in case 1. (4) An ERG (electron-releasing group, carbonium ion stabilizing) at C_α will exert a force in the direction of increased carbonium ion character if inserted into the transition-state geometry characteristic of some lesser ERG; therefore, in a given transition-state model, any normal mode which involves a change in carbonium ion character (corresponding to a component along the *diagonal* extending between the C^- and C^+ corners in Figure 1) will be increased or decreased, as described in case 1.

One further variable which is commonly probed in experiments on E2 reactions is π character. Increases in π character occur only when the C_β-H and C_α-X distances increase simultaneously. Therefore, π character increases along the diagonal extending from R to P corners in Figure 1 and could be estimated as the percentage of the distance from R toward P where the transition state is found. For transition states not lying on that diagonal, the π character is limited by that bond which is least broken and is estimated from the point where a vertical or a horizontal line drawn through the point representing the transition state intersects the diagonal. The correct estimate of π character is given by the vertical *or* horizontal line's intersection, whichever line intersects the diagonal closer to R. Thus, in the case of E1cB-like transition states (Figure 1, upper triangle), the extent of C_α-X bond breaking is less than C_β-H breaking, and C_α-X breaking determines the amount of π character. In this case, the π character is given by the intersection of a vertical line, dropped from the transition-state point, with the diagonal. Likewise, in the case of E1-like transition states (Figure 1, lower triangle), the extent of C_β-H breaking is less than C_α-X breaking, and C_β-H breaking now determines the amount of π character. In this case, the π character is given by the intersection of a horizontal line, drawn through the transition-state point, with the diagonal.

Predicted effects for the postulated central and the E1cB-like transition-state models can be derived, for each of the four cases of structural change described above. If the parallel and perpendicular contributions are approximately equal in magnitude,[5,16] then Figure 1, and the following predictions derived from it, result. The changes in transition-state structure shown in Figure 1 are exaggerated for visibility. For most real cases, the shift in transition-state structure caused by a given structural change would be expected to be smaller than, but in the same direction as, the diagram might imply.

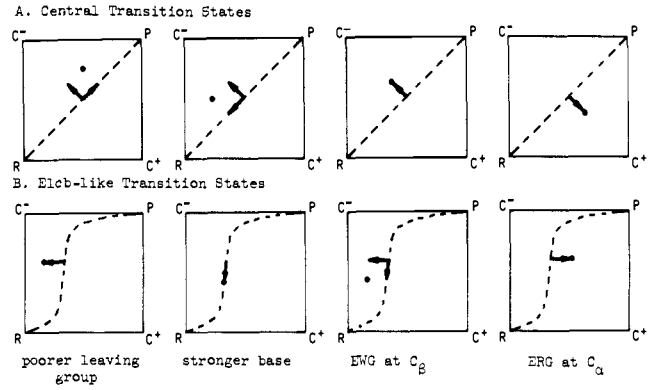

Figure 1. Schematic potential-energy surfaces[5,16] for E2 transition states described in text, showing reaction pathways as dashed lines, but omitting energy contours. R = reactant, P = product, C^- = carbanion (E1cB), and C^+ = carbonium ion (E1) geometries at the four corners. Abscissas and ordinates can be approximately visualized as C_α-X bond breaking and C_β-H bond breaking, respectively. It is assumed that (base) B-H bond making and C_α-C_β π-bond character parallel the breaking of the two bonds depicted reasonably closely. The unperturbed transition-state geometry discussed in the text is at the origin of the arrow(s). The arrows indicate the direction of the parallel (along the dashed line) and perpendicular effects predicted[5] (see also force formulation in text). The trend of the transition-state geometry for the structural change given in text is the resultant of the arrows, shown as a dot. Where only one arrow is shown, this results from the fact that the other effect, for which no arrow is shown, is predicted to be much smaller than that shown.

For the central transition state as above, a poorer leaving group should result in a longer C_β-H, little change in C_α-X, more carbanion character at C_β, and little change in π character; a stronger base should result in little change in C_β-H, a shorter C_α-X, more carbanion character at C_β, and a decrease in π character; an EWG at C_β should result in a longer C_β-H, a shorter C_α-X, more carbanion character at C_β, and a decrease in π character; an ERG at C_α should result in a shorter C_β-H, a longer C_α-X, less carbanion character at C_β or more carbonium ion character at C_α, and a decrease in π character.

For the E1cB-like transition state as above, a poorer leaving group should result in little change in C_β-H, a shorter C_α-X, more carbanion character at C_β, and a decrease in π character; a stronger base should result in a shorter C_β-H, little change in C_α-X, less carbanion character at C_β, and little change in π character; an EWG at C_β should result in a shorter C_β-H, a shorter C_α-X, little change in carbanion or carbonium ion character, and a decrease in π character; an ERG at C_α should result in little change in C_β-H, a longer C_α-X, less carbanion character at C_β, and an increase in π character.

The diagrams from which these effects were derived are shown in Figure 1. The reader will recognize that there are assumptions in these models; however, these are simply models which must be tested against experimental trends. At present, these models agree very well with known experimental trends, whereas other models (e.g., assumption of central or of E1cB-like transition states for all types of leaving group, or assumption that parallel effects will be inherently greater than perpendicular effects) do not. It will also

be noted that some of the diagrams in Figure 1 do not have two arrows, even though we have stated that we are assuming that parallel and perpendicular contributions are approximately equal in magnitude. This result comes from item 4 above. For example, in Figure 1, A(3), there is no arrow along the dashed line because this motion does not change the carbanion character at all. The assumption of equality of parallel and perpendicular contributions means that, where there *are* two arrows, we give them approximately equal lengths. Of course, this distinction is an approximation, but we believe that the *trends* are correctly derived in this way.

These predictions apply to the present isotope-effect results in the following way. The bromide and chloride leaving groups would have more central transition states, and the results show that the proton at C_β is half transferred, or less, to the lyoxide base. Changing to a more basic leaving group such as fluoride or ammonium is predicted above to cause a central transition state to have a longer C_β-H and more carbanion character. Thus, the more basic leaving group should shift the transition-state structure from central toward E1cB-like. The proton at C_β should be more transferred to lyoxide, as shown by the larger DO^-/HO^- isotope effects we have observed. If the transition state becomes highly E1cB-like in the sense of having a reaction-coordinate motion involving mainly proton transfer, as in Figure 1, then the above prediction is that there should be little change in C_β-H. Therefore, little change in proton transfer should take place upon making the leaving group more basic in an already E1cB-like transition state, and the DO^-/HO^- isotope effects should not change a great deal with leaving group. The more basic leaving groups, 'onium and fluoride, do in fact have similar isotope effects and thus also conform with prediction.

Justification for our conclusion that the agreement of these models with experiment is very good requires a comprehensive review of the extensive literature on E2 reactions. Numerous reviews and papers, which also contain further references, are available.[2-8,15,16] It is not possible to summarize the relevant data and interpretations concisely but, starting from the Saunders and Cockerill book,[2] which evaluates much of this information, it is possible to demonstrate agreement with the predictions above.

Experimental Section

Melting points were determined on a Thomas-Hoover melting-point apparatus and are corrected. Boiling points are uncorrected. Elemental analyses were generally performed by Alfred Bernhardt Microanalytisches Laboratorium im Max-Planck-Institut, West Germany. GLC was carried out with an Aerograph Model A-350-B gas chromatograph, using stainless steel columns 6-mm in diameter and helium flow of 60 ml/min.

β-(4-Nitrophenyl)ethyl Alcohol. Acetic anhydride (408 g, 4 mol) and sulfuric acid (reagent, 1.8 g) were combined in a flask cooled in an ice bath, and β-phenylethyl alcohol (366 g, 3 mol) was added while maintaining less than 25°. A mixture of acetic anhydride (935 g, 9.15 mol) and nitric acid (70% reagent, 293 g, 3.25 mol) was cooled in a flask to −15° using an acetone–Dry Ice bath, and the former solution was added in 1 hr while maintaining less than 5°, kept at 0–5° 1 more hr, poured into 2 kg of ice, and the oil was extracted with 2 l. of benzene. The benzene solution was washed with 5% aqueous sodium hydroxide, washed with water until neutral, dried over magnesium sulfate, and filtered, and the solvent was removed on a rotary evaporator, giving crude (ortho and para isomers) β-nitrophenylethyl acetate (620 g, 99%). The crude acetate was dissolved in 1 l. of anhydrous methanol, anhydrous hydrogen chloride (15 g, 0.41 mol) added, and the solution allowed to stand at 25° for 48 hr. After evaporation of solvent, partial crystallization took place in the refrigerator (ca. 2°). The solid was isolated by filtration, giving after two recrystallizations from ethanol–water (60–40 mol) pure para isomer (178.5 g, 36%), mp 61–62° (lit.[18] mp 60°).

Anal. Calcd for $C_8H_9NO_3$: C, 57.48; H, 5.43; N, 8.38. Found:[19] C, 57.37; H, 5.47; N, 8.30.

β-(4-Dimethylaminophenyl)ethyl Alcohol. Into the reaction bottle of a Paar hydrogenation apparatus was charged β-(4-nitrophenyl)ethyl alcohol (33.2 g, 0.2 mol), ethanol (200 ml), 37% aqueous formaldehyde (64.8 g, 0.8 mol), and 5% palladium on powdered charcoal (7.5 g). Air was removed by several pressure-vent cycles with hydrogen, the bottle pressurized to 55 psig, and the pressure maintained at >20 psig until absorption was complete, in 3–4 hr. Filtration and evaporation of solvent gave crude product (nearly quantitative). Crude products from three reductions were combined and extracted into refluxing hexane, then carefully decanted from residual oil. Cooling of the hexane solution and filtration gave β-(4-dimethylaminophenyl)ethyl alcohol (52 g, 52.5%), mp 57–58°, showing a single peak on GLC (60-cm 20% SE-30 silicone rubber on Chromosorb-W 175°) which was clearly separated from starting material.

Anal. Calcd for $C_{10}H_{15}NO$: C, 72.69; H, 9.15; N, 8.48. Found:[19] C, 72.71; H, 9.15; N, 8.58.

The same reduction procedure, but starting with commercial β-(4-aminophenyl)ethyl alcohol, gave a compound identical in GLC, infrared, melting point, and mixture melting point with the above compound.

β-(4-Dimethylaminophenyl)ethyl Chloride. β-(4-Dimethylaminophenyl)ethyl alcohol (16.5 g, 0.1 mol) was added slowly to thionyl chloride (bp 75.5–76.5°, 17.9 g, 0.15 mol) while maintaining <20° by cooling in an ice bath, allowed to stand at 25° for 12 hr, heated at 60° for 30 min, cooled and poured into 50 ml of anhydrous ethanol (with rapid evolution of gases). Removal of solvent with a rotary evaporator gave crude amine hydrochloride (22 g, 100%), which was dissolved in water and made basic with sodium carbonate, the oil was extracted into benzene, the benzene solution washed with water, dried over magnesium sulfate, the benzene evaporated, and the residue fractionated under reduced pressure, giving colorless product, 9.0 g, 49%, bp 85.5–86° (0.15 mm), showing a single peak on GLC (60-cm 10% Carbowax 20M on Chromosorb W, 205°).

Anal. Calcd for $C_{10}H_{14}ClN$: C, 65.39; H, 7.68; Cl, 19.30; N, 7.63. Found:[19] C, 65.45; H, 7.65; Cl, 19.33; N, 7.68.

4-(2-Chloroethyl)phenyltrimethylammonium Tosylate. β-(4-Dimethylaminophenyl)ethyl chloride (5.0 g, 27 mmol) and methyl tosylate (9.3 g, 50 mmol) were combined in benzene (50 ml) and allowed to stand at 25° for 96 hr, and the precipitated solid was collected, vacuum dried, mp 217–218° dec, and recrystallized from ethanol–benzene to constant mp 217–218° dec. Additional product, up to a 100% crude yield after 2 months, could be isolated from the mother liquor.

Anal. Calcd for $C_{18}H_{24}ClNO_3S$: C, 58.47; H, 6.54; Cl, 9.58; N, 3.79; S, 8.67. Found:[19] C, 58.46, 58.50; H, 6.59, 6.55; Cl, 9.40, 9.53; N, 3.84, 3.81; S, 8.74, 8.80.

β-(4-Dimethylaminophenyl)ethyl Bromide. This compound was prepared in essentially the same way as the corresponding chloride, above, using thionyl bromide,[20] except that, after addition, the reaction mixture was heated at 70° for 2 hr and allowed to stand for 12 hr, giving crude, solid product (22.5 g, 98%), which was recrystallized twice from hexane, to give 12 g, 53%, mp 45–46°, showing a single peak on GLC (60-cm 10% Carbowax 20M on Chromosorb W, 175°).

Anal. Calcd for $C_{10}H_{14}BrN$: C, 52.65; H, 6.18; Br, 35.03; N, 6.14. Found: C, 52.73; H, 6.16; Br, 35.02; N, 6.17.

4-(2-Bromoethyl)phenyltrimethylammonium Tosylate. This compound was prepared in the same way as the corresponding chloro compound (see above). After standing for 18 days at 25°, filtration gave 90% of crude product, which was recrystallized from ethanol–benzene to constant mp 204.5–205.0° dec, yield 80%.

Anal. Calcd for $C_{18}H_{24}BrNO_3S$: C, 52.18; H, 5.84; Br, 19.28; N, 3.38; S, 7.74. Found:[19] C, 52.32, 52.14; H, 6.02, 5.91; Br, 19.13, 19.25; N, 3.37, 3.26; S, 7.63, 7.66.

β-(4-Dimethylaminophenyl)ethyltrimethylammonium Tosylate. To a solution of β-(4-dimethylaminophenyl)ethyl alcohol (16.5 g, 0.10 mol) and triethylamine (11.2 g, 0.11 mol) in benzene (50 ml) was added slowly *p*-toluenesulfonyl chloride (19.0 g, 0.10 mol) in benzene (50 ml). The reaction temperature reached 40° in about 45 min, after which stirring was continued for 8 hr. After filtration to remove triethylamine hydrochloride, the benzene solution was cooled, anhydrous trimethylamine (39 g, 0.66 mol) added, the so-

lution refrigerated for 5 days, and the crude product (20 g, 53%) isolated by filtration and recrystallized from ethanol–ether, giving 12.9 g, 34%, of white solid, mp 244–245° dec.

Anal. Calcd for $C_{20}H_{30}N_2O_3S$: C, 63.46; H, 7.99; N, 7.40; S, 8.47. Found: C, 63.32; H, 7.96; N, 7.49; S, 8.55.

β-(4-Trimethylammoniophenyl)ethyltrimethylammonium Ditosylate. To a solution of β-(4-dimethylaminophenyl)ethyltrimethylammonium tosylate (10 g, 26 mmol) in absolute methanol (55 ml) was added methyl tosylate (18.6 g, 100 mmol) and the solution heated at reflux for 10 hr. The precipitated salt was isolated by filtration and extracted several times with boiling methanol, giving 11.0 g, 74.4%, of white crystals, mp >330°.

Anal. Calcd for $C_{28}H_{40}N_2O_6S_2$: C, 59.55; H, 7.14; N, 4.96; S, 11.35. Found: C, 59.63, 59.49; H, 7.02, 7.19; N, 4.91, 4.86; S, 11.13, 11.26.

4-(2-Tosyloxyethyl)phenyltrimethylammonium Tosylate. The preparation was carried out as for β-(4-dimethylaminophenyl)ethyltrimethylammonium tosylate, except that methyl tosylate (46.5 g, 0.25 mol) was added, instead of trimethylamine, to the uncooled solution, and the mixture was then stirred for 96 hr at 25°. The solid precipitate was isolated by filtration, dried, and recrystallized from acetonitrile–ethanol (10/1, v/v), giving 18.0 g, 36%, mp 199–201°.

Anal. Calcd for $C_{25}H_{31}NO_6S_2$: C, 59.38; H, 6.18; N, 2.77; S, 12.68. Found: C, 59.29; H, 6.28; N, 2.73; S, 12.79.

β-(4-Trimethylammoniophenyl)ethyldimethylsulfonium Ditosylate. 4-(2-Tosyloxyethyl)phenyltrimethylammonium tosylate (15.0 g, 30 mmol) was dissolved in dimethylformamide (250 ml, dried over molecular sieves) and added to a pressure bottle which was then cooled in an ice bath and dimethyl sulfide (40.6 g, 0.65 mol) added. The bottle was sealed and placed in an oil bath at 80–85° for 96 hr and the precipitate isolated by filtration and washed with dimethylformamide and then hot benzene, giving 8.2 g, 48%, mp 255–256° dec.

Anal. Calcd for $C_{27}H_{37}NO_6S_3$: C, 57.12; H, 6.57; N, 2.47; S, 16.94. Found: C, 57.05, 57.19; H, 6.42, 6.43; N, 2.45, 2.32; S, 17.08, 17.10.

Phenyl-β-(4-dimethylaminophenyl)ethylmethylamine.[21] To magnesium (3.86 g, 0.16 mol) in anhydrous ether (75 ml) was slowly added, with stirring, a solution of isopropyl bromide (18.8 g, 0.15 mol) in anhydrous ether (75 ml), the solution stirred for 3 hr, a solution of *N*-methylaniline (laboratory redistilled, 16.1 g, 0.15 mol) in anhydrous ether (50 ml) slowly added, with vigorous gas evolution, and then the ether distilled off under vacuum and benzene (reagent grade, used without further drying, 150 ml) added to dissolve the residue. β-(4-Dimethylaminophenyl)ethyl bromide (34.2 g, 0.15 mol) in benzene (50 ml) was added, the reaction mixture refluxed for 14 hr, the benzene solution filtered from the insoluble magnesium bromide, which was extracted with fresh benzene, the combined benzene solutions were washed several times with water, dried over magnesium sulfate, the benzene was removed on a rotary evaporator, and the residue fractionally distilled, giving light yellow product (11.6 g, 30%), bp 154–155° (0.15 mm), which solidified on cooling, mp 59–61°.

Anal. Calcd for $C_{17}H_{22}N_2$: C, 80.27; H, 8.72; N, 11.01. Found: C, 80.08; H, 8.71; N, 10.82.

β-(4-Trimethylammoniophenyl)ethylphenyldimethylammonium Ditosylate. Phenyl-β-(4-dimethylaminophenyl)ethylmethylamine (10.2 g, 40 mmol) and methyl tosylate (46.5 g, 0.25 mol) were refluxed in methanol (100 ml) for 70 hr, and the crude product was isolated by precipitation with ether, appearing to be a mixture (wide melting range) of mono- and bis quaternary salts. Upon solution in ethanol and cooling to 25°, the desired bis salt was isolated, mp 240–242°, while the mono salt was recovered at 0°, mp 175–178°. The bis salt was recrystallized to constant mp, 244.5–245.5°, yield 6.5 g, 26%.

Anal. Calcd for $C_{33}H_{42}N_2O_6S_2$: C, 63.23; H, 6.75; N, 4.47; S, 10.23. Found: C, 63.16, 63.10; H, 6.78, 6.68; N, 4.26, 4.36; S, 10.26, 10.10.

β-Phenylethyl Fluoride.[22] A slurry of potassium fluoride (174.3 g, 3.0 mol) in anhydrous diethylene glycol (500 g) was heated to 140–145° under a vacuum (50 mm). β-Phenylethyl bromide (277.6 g, 1.5 mol) was added from a pressure-equalizing funnel at a rate such that distillate temperature did not exceed 95° (4 hr). The distillate (135 g) was dissolved in 200 ml of benzene and washed with 5% aqueous sodium hydroxide, washed neutral with water, and dried over magnesium sulfate. Analysis by GLC (60-cm 10% Carbowax 20M on Chromosorb W, 135°) showed two major peaks in addition to a small amount of starting bromide. The impurity was styrene as shown by comparison with an authentic sample and disappearance of this material upon treatment with bromine. Careful fractionation on a 60-cm metal-packed, vacuum-jacketed column gave cuts which were substantially enriched in fluoride; these cuts were combined and dissolved in benzene, the solution was cooled in an ice bath, bromine added until its color remained for 5 min, and the solution washed with dilute sodium carbonate, then water, and dried over magnesium sulfate, giving upon distillation pure fluoride, bp 83–84° (50 mm) [lit.[22] bp 55–56° (12 mm)].

β-(4-Nitrophenyl)ethyl Fluoride. To a solution of nitric acid (70% reagent, 35.1 g, 0.39 mol) in acetic anhydride (102 g, 1.0 mol) at −10 to 0° was added slowly β-phenylethyl fluoride (34.0 g, 0.27 mol), the reaction mixture held at 0–5° for 3 hr after addition was complete, then poured into ice, extracted with benzene, the benzene solution washed several times with water, then with 10% aqueous sodium carbonate, then with water to neutrality, dried with magnesium sulfate, and the benzene removed on a rotary evaporator, giving 41.5 g, 89%, of an oil which partially crystallized on cooling, a mixture of ortho and para isomers, separated on analytical GLC (60-cm 10% Carbowax 20M on Chromosorb W, 200°). The solids were collected, yield 18 g, and considerable para isomer was also recovered by distillation of the liquid [ortho: bp 65–69° (0.20 mm), 9.0 g; para: bp 73–76° (0.20 mm), 9.3 g]. The combined para isomer was recrystallized from hexane–ethanol (90/10 v/v), giving 15 g, 33%, mp 47–48.5°.

Anal. Calcd for $C_8H_8FNO_2$: C, 56.80; H, 4.76; F, 11.23; N, 8.28. Found: C, 56.92; H, 4.88; F, 11.42; N, 8.30.

β-(4-Dimethylaminophenyl)ethyl Fluoride. This compound was prepared from β-(4-nitrophenyl)ethyl fluoride (12.0 g, 0.071 mol), ethanol (175 ml), 37% aqueous formaldehyde (24.3 g, 0.30 mol), and 5% palladium on powdered charcoal (5.0 g) in essentially the same way described above for β-(4-dimethylaminophenyl)ethyl alcohol, with pressurization to 63 psig and completion of absorption of hydrogen in 1–2 hr. After filtration, evaporation of the solvent gave a nearly quantitative yield of crude product, which was dissolved in benzene, washed with 5% aqueous sodium hydroxide, washed neutral with water, dried over magnesium sulfate, and distilled, giving the product, bp 51–53° (0.10 mm), 8.6 g, 72%.

Anal. Calcd for $C_{10}H_{14}FN$: C, 71.82; H, 8.44; F, 11.36; N, 8.38. Found: C, 71.85; H, 8.27; F, 11.28; N, 8.50.

4-(2-Fluoroethyl)phenyltrimethylammonium Tosylate. β-(4-Dimethylaminophenyl)ethyl fluoride (6.7 g, 0.04 mol) and methyl tosylate (30 g, 0.16 mol) were combined in benzene (125 ml) and stirred for 11 days. The precipitated solid was isolated and vacuum dried, yield 98%, then recrystallized from anhydrous ethanol to constant mp 216–217.5°.

Anal. Calcd for $C_{18}H_{24}FNO_3S$: C, 61.17; H, 6.84; F, 5.38; N, 3.96; S, 9.07. Found: C, 61.04, 61.25; H, 6.77, 6.94; F, 5.71, 5.53; N, 3.88, 3.80; S, 8.94, 8.89.

***N,N*-Dimethyl-4-vinylaniline.** To β-(4-dimethylaminophenyl)ethyl bromide (20 g, 88 mmol) in absolute ethanol (100 ml) with *N,N'*-diphenyl-*p*-phenylenediamine (20 mg) as a polymerization inhibitor was added 0.5 *N* potassium hydroxide in ethanol (400 ml) and the solution heated at 60° for 3 hr, filtered to remove potassium bromide, and the ethanol removed with a rotary evaporator. The residue was dissolved in benzene, washed neutral with water, dried over magnesium sulfate, and the solvent removed, giving crude product which showed three peaks on GLC (60-cm 15% SE-30 silicone rubber on Chromosorb W, 150°). Two fractional distillations gave pure product, bp 57–58° (0.25 mm), yield 4.3 g, 33%, mp 15–16° (lit.[23] mp 16–16.8°; 15–17°).

Anal. Calcd for $C_{10}H_{13}N$: C, 81.59; H, 8.90; N, 9.52. Found: C, 81.43; H, 8.73; N, 9.64.

4-Vinylphenyltrimethylammonium Tosylate. *N,N*-Dimethyl-4-vinylaniline (2.50 g, 17 mmol) and methyl tosylate (12.6 g, 68 mmol) were combined in benzene (25 ml), giving after 11 days at 25° a quantitative yield of crude product, which was recrystallized from small amounts of anhydrous ethanol to constant mp 203–205° and constant molar absorptivity, λ_{max} 249 nm, ϵ_{max} 16,800.

Anal. Calcd for $C_{18}H_{23}NO_3S$: C, 64.85; H, 6.95; N, 4.20; S, 9.60. Found: C, 64.64; H, 6.82; N, 4.15; S, 9.71.

Kinetic Procedures. Kinetic and product studies were carried out

essentially as described previously,[1a] using HO^- in H_2O and DO^- in D_2O, with the following differences. A 2.5-ml RGI, Inc., ultraprecision micrometer buret was used for titration with standard hydrochloric acid. The indicator was Neutral Red–Methylene Blue except with phenoxide solutions, in which case Bromocresol Purple was used. All kinetic runs were carried out in flasks made of alkali-resistant glass (Corning Glass No. 7280), sealed with a needle puncture stopper. Aliquots, taken with a syringe, were 2 ml and were measured gravimetrically for each point. The bath temperature was 60.00 ± 0.005° (NBS Certified thermometer).

Olefin yields were 100 ± 4% (crosschecked with two different ultraviolet spectrophotometers), with the exception of the reaction of 4-(2-bromoethyl)phenyltrimethylammonium tosylate with phenoxide, in which case olefin yields were used to calculate percentage of E2 and SN2 processes.

Acknowledgments. Support by the National Science Foundation is gratefully acknowledged.

References and Notes

(1) (a) Previous paper: L. J. Steffa and E. R. Thornton, *J. Am. Chem. Soc.*, **89**, 6149 (1967); (b) supported in part by the National Science Foundation through Grants GP-2937, GP-6047, and GP-34,491X; (c) for further details, cf. D. A. Winey, Ph.D. Dissertation in Chemistry, University of Pennsylvania, 1968.
(2) W. H. Saunders, Jr., and A. F. Cockerill, "Mechanisms of Elimination Reactions", Wiley, New York, N.Y., 1973.
(3) J. F. Bunnett, *Angew. Chem., Int. Ed. Engl.*, **1**, 225 (1962).
(4) J. F. Bunnett in "Survey of Progress in Chemistry", Vol. 5, A. F. Scott, Ed., Academic Press, New York, N.Y., 1969, p 53.
(5) R. A. More O'Ferrall, *J. Chem. Soc. B*, 274 (1970).
(6) A. Fry, *Chem. Soc. Rev.*, **1**, 163 (1972).
(7) F. G. Bordwell, *Acc. Chem. Res.*, **5**, 374 (1972).
(8) W. T. Ford, *Acc. Chem. Res.*, **6**, 410 (1973).
(9) F. H. Westheimer, *Chem. Rev.*, **61**, 265 (1961).
(10) See, for example, E. K. Thornton and E. R. Thornton in "Isotope Effects in Chemical Reactions", C. J. Collins and N. S. Bowman, Ed., Van Nostrand-Reinhold, New York, N.Y., 1970, Chapter 4.
(11) C. G. Swain and A. S. Rosenberg, *J. Am. Chem. Soc.*, **83**, 2154 (1961).
(12) L. Pentz and E. R. Thornton, *J. Am. Chem. Soc.*, **89**, 6931 (1967).
(13) R. L. Schowen, *Prog. Phys. Org. Chem.*, **9**, 275 (1972).
(14) E. R. Thornton, *J. Am. Chem. Soc.*, **89**, 2915 (1967).
(15) R. A. Bartsch and J. F. Bunnett, *J. Am. Chem. Soc.*, **91**, 1376, 1382 (1969).
(16) P. J. Smith and A. N. Bourns, *Can. J. Chem.*, **52**, 749 (1974).
(17) W. P. Jencks, *Chem. Rev.*, **72**, 705 (1972).
(18) S. T. Rashevskaya, E. S. Kashcheeva, and E. I. Mostoslavskaya, *Zh. Obshch. Khim.*, **33**, 3998 (1963).
(19) Micro-Analysis, Inc., Wilmington, Del.
(20) Prepared by the method of R. C. Elderfield, W. J. Gensler, F. Brady, J. D. Head, S. C. Dickerman, L. Wiederhold, III, C. B. Kremer, H. A. Hageman, F. J. Kreysa, J. M. Griffins, S. M. Kupchan, B. Newman, and J. T. Maynard, *J. Am. Chem. Soc.*, **68**, 1579 (1946).
(21) Procedure adapted from M. S. Kharasch, G. H. Williams, and W. Mudenberg, *J. Org. Chem.*, **20**, 937 (1955).
(22) C. H. DePuy and C. A. Bishop, *J. Am. Chem. Soc.*, **82**, 2535 (1960).
(23) (a) R. W. Strassburg, R. A. Gregg, and C. Malling, *J. Am. Chem. Soc.*, **69**, 2141 (1947); (b) E. Selegny, *Bull. Soc. Chim. Fr.*, 1275 (1959).

Influence of Solvent on the Motion of Molecules "Immobilized" on Polystyrene Matrices and on Glass Surfaces[1]

Steven L. Regen

Contribution from the Department of Chemistry, Marquette University, Milwaukee, Wisconsin 53233. *Received December 5, 1974*

Abstract: The influence of solvent on the rotational motion of 2,2,6,6-tetramethyl-4-piperidinol-1-oxyl (**1**) covalently bound to cross-linked polystyrene, silica, and a polystyrene ion-exchange resin has been examined by electron paramagnetic resonance spectroscopy. The degree of swelling of the polymer supports, as defined by the solvent employed, is an important factor in determining the mobility of the attached spin label. In contrast, when immobilized on a rigid silica surface, the motion of **1** is considerably less sensitive to the nature of the solvent. Evidence is presented which suggests that hydrogen-bonding forces may be important in influencing the physical properties of molecules immobilized on silica.

Glass surfaces show considerable promise as support material for enzymes.[2] The successful application of polystyrene resins to organic synthesis,[3] transition-metal catalysis,[4] and photochemistry[5] suggests that silica may find similar use.[6] Until recently, little attention has been given to the role which the solvent plays in the chemistry of substrates "immobilized" on insoluble supports. It is now evident that the choice of solvent can have a dominant influence on the physical nature of molecules bound to polystyrene matrices, and that the primary function of the solvent is to define the degree of swelling of the polymer lattice.[7,8] Recent studies dealing with polymer-bound transition-metal catalysts and complexes strongly suggest that swelling is also an important factor in determining the chemical reactivity of immobilized molecules.[9] Silica, unlike polystyrene, is rigid and is not subject to swelling. One might expect that for molecules bound to this type of lattice, the choice of solvent would be of little consequence to their physical and, possibly, chemical behavior. Such a property could represent a subtle but important advantage of silica over polystyrene as support material.

The work reported in this paper was carried out in order to provide a basis for understanding how solvent influences the physical nature of molecules bonded to silica and to polystyrene supports. The approach which we have taken was based on the spin-labeling technique, where we have examined the rotational motion of a nitroxide radical attached to solvent-swelled 2% cross-linked polystyrene and to solvent-wetted silica.[10]

Results and Discussion

Attachment to a Polystyrene Matrix. The nitroxide 2,2,6,6-tetramethyl-4-piperidinol-1-oxyl (**1**) was covalently attached to polystyrene by reaction of its sodium salt with 2% cross-linked chloromethylated polystyrene **2** to yield nitroxide–polystyrene **3**.

The room-temperature electron paramagnetic resonance (EPR) spectrum of **3** in the dry state exhibited a "powder" spectrum indicating slow rotational motion (Figure 1A). Swelling **3** with carbon tetrachloride caused a large increase in the rotational motion of the nitroxide moiety as evidenced by the change in the EPR spectrum (Figure 1C).